

Supporting Information

for

**Preference of halogen bonds over hydrogen bonds within a discrete  
three-component co-crystal that undergo a [2 + 2] cycloaddition  
reaction**

Conrad J. Powell, Eric Bosch, Herman R. Krueger, Jr.,  
and Ryan H. Groeneman

Department of Biological Sciences, Webster University, St. Louis, MO, 63119, USA

Department of Chemistry, Missouri State University, Springfield, MO 65804, USA

1. Materials, General Methods and Synthesis of the Co-crystals	Page 2
2. Electronic Structure Calculations	Page 3
3. Single X-ray Diffraction Information and Data Tables	Page 4-5
4. <sup>1</sup> H NMR Spectroscopic Data	Page 6-7
5. Powder X-ray Diffractograms	Page 8-10

## 1. Materials, General Methods and Synthesis of the Co-crystals

### Materials

*trans*-1,2-bis(4-pyridyl)ethylene (**BPE**), 4,4'-azopyridine (**AP**), and the solvent toluene were both purchased from Sigma-Aldrich Chemical (St. Louis, MO, USA) and used as received. 1,2-bis(4-pyridyl)acetylene (**BPA**) was purchased from Synquest Laboratories (Alachua, FL, USA) and used as received. The halogen bond donor 1,2,4,5-tetrachloro-3-iodobenzene ( $C_6HI_4$ ) was synthesized from 2,3,5,6-tetrachloroaniline by a sequential diazotization-iodination procedure previously reported for the synthesis of 1,3,5-trichloro-2-iodobenzene from 2,4,6-trichloroaniline.<sup>1</sup> All crystallization studies were performed in 20 mL scintillation vials.

### General Methods

Photoreactions were conducted using UV-radiation from a 450 W medium-pressure mercury lamp in an ACE Glass photochemistry cabinet. The co-crystals  $2(C_6HI_4) \cdot (BPE)$  was placed between a pair of Pyrex glass plates for irradiation. The photoreactivity of  $2(C_6HI_4) \cdot (BPE)$  was determined after exposure to UV light by using  $^1H$  NMR spectroscopy.  $^1H$  NMR spectrum was collected using a Bruker Avance 400 MHz spectrometer using  $DMSO-d_6$  as a solvent. Powder X-ray diffraction data was collected at room temperature on a Bruker D8 Advance X-ray diffractometer using  $Cu K_{\alpha}$  radiation ( $\lambda = 1.54059 \text{ \AA}$ ) between  $5^\circ$  to  $40^\circ$  two-theta.

### Synthesis of $2(C_6HI_4) \cdot (BPE)$

Co-crystals of  $2(C_6HI_4) \cdot (BPE)$  were synthesized by dissolving 50.0 mg of  $C_6I_5$  in 2.0 mL of toluene, which was then combined with a separate 2.0 mL toluene solution containing 13.3 mg of **BPE** (2:1 molar equivalent). The solutions were mixed and allowed to slowly evaporate. Within two days crystals suitable for X-ray diffraction were formed.

### Synthesis of $2(C_6HI_4) \cdot (BPA)$

Co-crystals of  $2(C_6HI_4) \cdot (BPA)$  were synthesized by dissolving 50.0 mg of  $C_6I_5$  in 2.0 mL of toluene, which was then combined with a separate 2.0 mL toluene solution containing 13.2 mg of **BPA** (2:1 molar equivalent). The solutions were mixed and allowed to slowly evaporate. Within two days crystals suitable for X-ray diffraction were formed.

### Synthesis of $2(C_6HI_4) \cdot (AP)$

Co-crystals of  $2(C_6HI_4) \cdot (AP)$  were synthesized by dissolving 50.0 mg of  $C_6I_5$  in 2.0 mL of toluene, which was then combined with a separate 2.0 mL toluene solution containing 13.4 mg of **AP** (2:1 molar equivalent). The solutions were mixed and allowed to slowly evaporate. Within two days crystals suitable for X-ray diffraction were formed.

## 2. Electronic Structure Calculations

To obtain binding energies, Density Functional Theory calculations were performed using the M06-2X density functional as implemented in the Gaussian 16 program.<sup>2</sup> X-ray diffraction data was used to determine the positions of all atoms, with the exception of hydrogen. The hydrogen coordinates were obtained by performing a molecular mechanics<sup>3</sup> optimization with all non-hydrogen atoms frozen at the X-ray diffraction values. An aug-cc-pVTZ basis set, stored internally in the Gaussian program, was used for all atoms, with the exception of iodine. In the case of iodine, an aug-cc-pVTZ basis set, which included a core potential replacing the inner 28 electrons, was obtained from the EMSL Basis Set Exchange Library.<sup>4</sup> The energies were computed using the counterpoise method as implemented in Gaussian. This procedure computes the energy as the difference between the energy of the pair and the energies of the separated molecules. In the case of the separated fragments, the energies are computed using the entire set of orbitals for the molecular pair. For all calculations, the counterpoise correction was rather modest, comprising no more than about 10% of the computed value.

### 3. Single X-ray Diffraction Information and Data Tables

X-ray data was collected on a Rigaku XtaLAB Synergy diffractometer using Cu K $\alpha$  radiation ( $\lambda = 1.54184 \text{ \AA}$ ) with a HyPix detector. Crystals were immersed in Paratone oil, and a suitable specimen placed on a MiTeGen mount. The data was collected at ambient temperature. An analytical numerical absorption correction was applied within CrysAlis<sup>Pro</sup><sup>5</sup> using a multifaceted crystal model based on expressions derived by Clark and Reid.<sup>6</sup> The structures were solved in Olex2<sup>7</sup> with the SHELXT<sup>8</sup> structure solution program using Intrinsic Phasing and refined with the olex2.refine<sup>9</sup> refinement package using Gauss-Newton minimization. In all structures hydrogen atoms bound to carbon atoms were located in the difference Fourier map and were geometrically constrained using the appropriate AFIX commands. In the co-crystal 2(C<sub>6</sub>HICl<sub>4</sub>)•(BPE), the alkene group was modelled over two positions with the help of a free variable. The relative populations refined as 0.81:0.19. A distance restraint, C3-C6A = 1.49(2) Å, for the pyridine C-alkene C distance corresponding to the minor component. EADP was applied to the unique alkene C of both disorder components. In the co-crystal 2(C<sub>6</sub>HICl<sub>4</sub>)•(AP), the azo group was modelled over two positions that refined with a free variable to 0.51:0.49. In this structure the pyridine C connected to the azo linkage was also modelled over two positions with the same free variable. The distance restraint DFIX was set to 1.43(2) Å for C5-N2 and C5A-N2A. Further modelling of the rest of the pyridyl group was not productive and the displacement ellipsoids for C1 and C4 are accordingly elongated.

**Table S1.** X-ray data for 2(C<sub>6</sub>HICl<sub>4</sub>)•(BPE), 2(C<sub>6</sub>HICl<sub>4</sub>)•(BPA), and 2(C<sub>6</sub>HICl<sub>4</sub>)•(AP).

crystal code	2(C <sub>6</sub> HICl <sub>4</sub> )•(BPE)	2(C <sub>6</sub> HICl <sub>4</sub> )•(BPA)	2(C <sub>6</sub> HICl <sub>4</sub> )•(AP)
chemical formula	C <sub>24</sub> H <sub>12</sub> Cl <sub>8</sub> I <sub>2</sub> N <sub>2</sub>	C <sub>24</sub> H <sub>10</sub> Cl <sub>8</sub> I <sub>2</sub> N <sub>2</sub>	C <sub>24</sub> H <sub>10</sub> Cl <sub>8</sub> I <sub>2</sub> N <sub>4</sub>
formula mass	865.81	863.79	867.78
crystal system	monoclinic	monoclinic	monoclinic
space group	<i>P2<sub>1</sub>/c</i>	<i>P2<sub>1</sub>/c</i>	<i>P2<sub>1</sub>/c</i>
a/Å	4.0650(1)	4.0163(1)	4.0199(1)
b/Å	11.0283(2)	11.2938(1)	10.882(3)
c/Å	32.1854(6)	31.5449(4)	32.3284(10)
α/°	90	90	90
β/°	91.484(2)	91.831(1)	91.490(3)
γ/°	90	90	90
V/Å <sup>3</sup>	1442.39(5)	1430.12(4)	1414.52(7)
ρ <sub>calc</sub> /g cm <sup>-3</sup>	1.994	2.006	2.037
T/K	299	298	298
Z	2	2	2
radiation type	Cu Kα, 1.54184 Å	Cu Kα, 1.54184 Å	Cu Kα, 1.54184 Å
absorption coefficient, μ/mm <sup>-1</sup>	24.11	24.31	24.61
no. of reflections measured	14136	14488	12094
no. of independent reflections	3100	2900	3011
R <sub>int</sub>	0.050	0.045	0.072
R <sub>1</sub> (I > 2σ(I))	0.0433	0.0330	0.0673
wR(F <sup>2</sup> ) (I > 2σ(I))	0.1167	0.0874	0.1769
R <sub>1</sub> (all data)	0.0467	0.0725	0.0725
wR(F <sup>2</sup> ) (all data)	0.1200	0.0893	0.1800
Goodness-of-fit	1.0332	1.0274	1.0385
CCDC deposition number	2264915	2264916	2264917

#### 4. $^1\text{H}$ NMR Spectroscopic Data

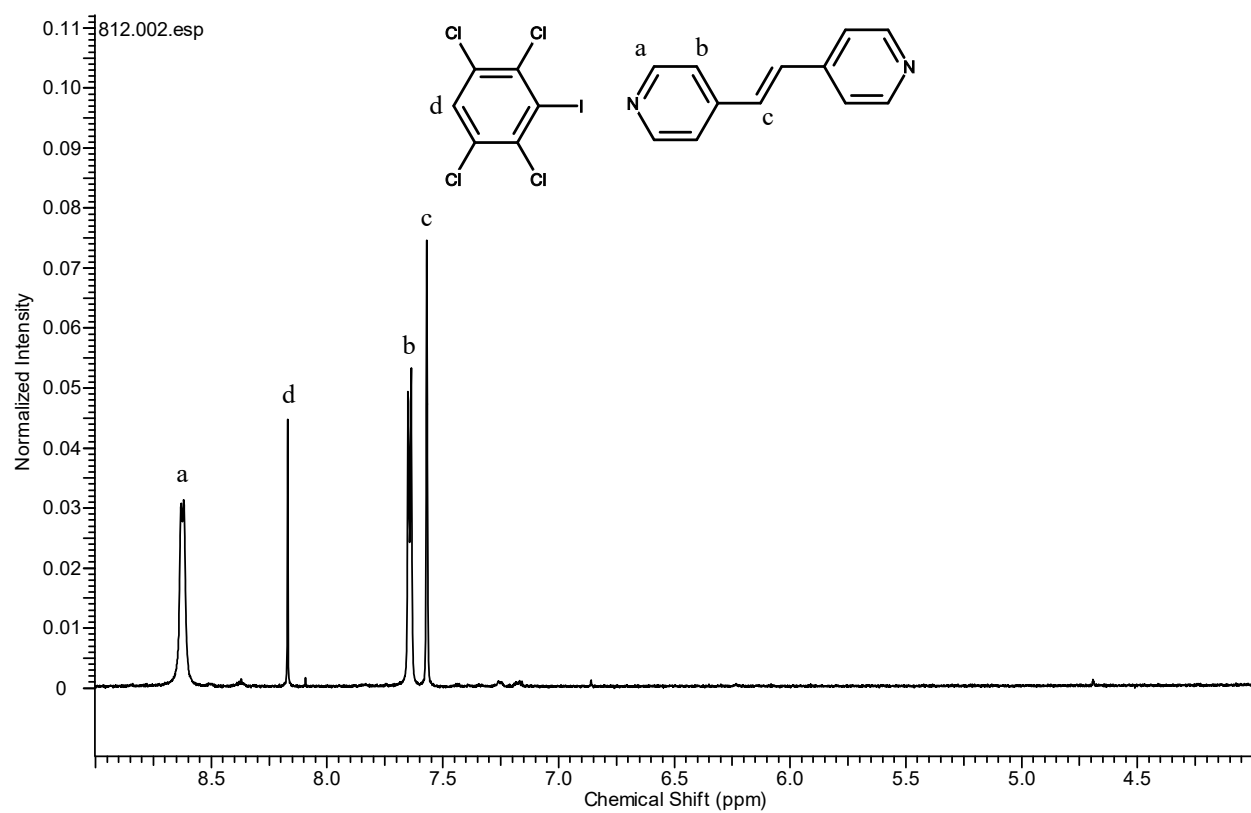


**Figure S1:**  $^1\text{H}$  NMR spectrum of the co-crystal  $(\text{C}_6\text{HICl}_4) \cdot (\text{BPE})$  before UV irradiation (400 MHz,  $\text{DMSO-}d_6$ ).

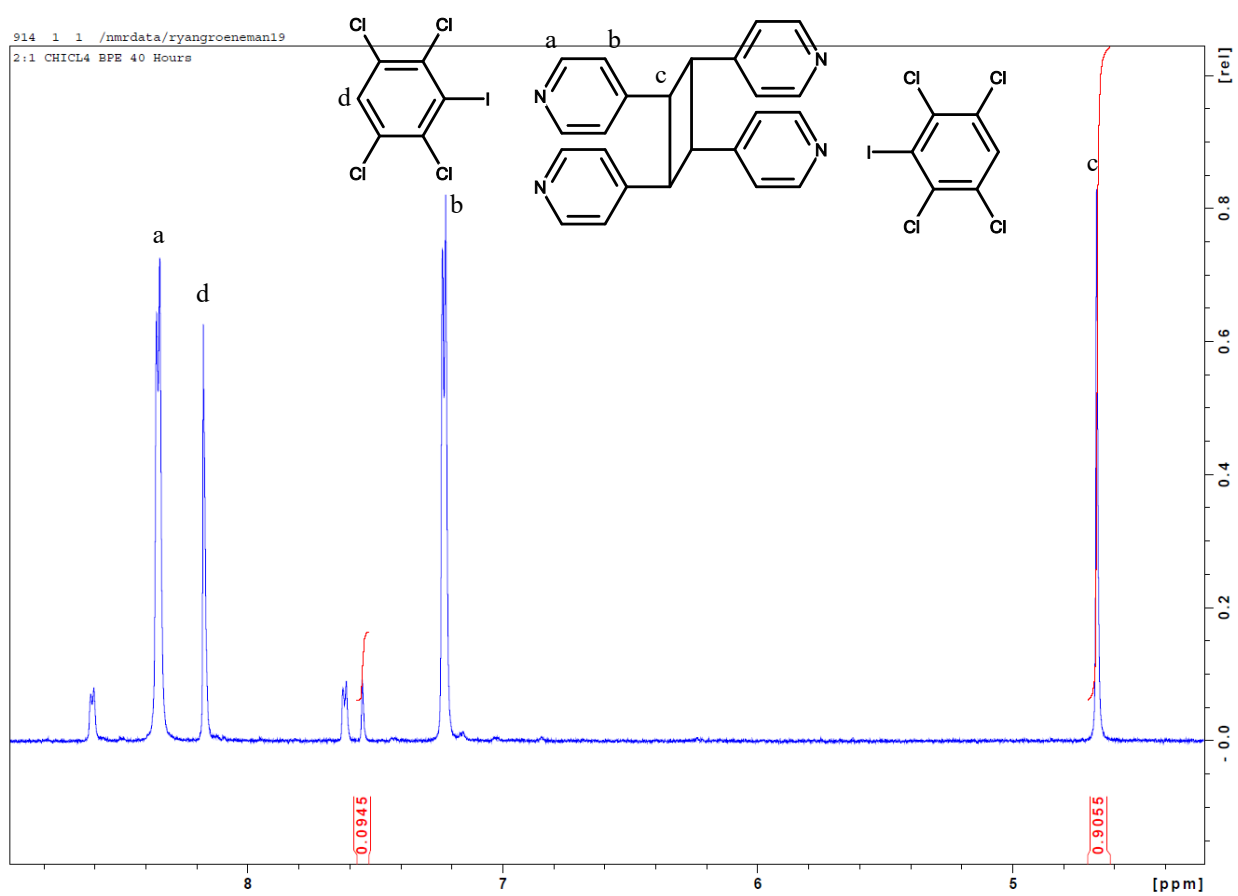


**Figure S2:**  $^1\text{H}$  NMR spectrum of  $(\text{C}_6\text{HICl}_4)\cdot(\text{TPCB})$  after 40 hours of UV irradiation reaching a yield of 91% for the [2 + 2] cycloaddition reaction for the solid from the fast evaporation rate (400 MHz,  $\text{DMSO}-d_6$ ).

## 5. Powder X-ray Diffractograms

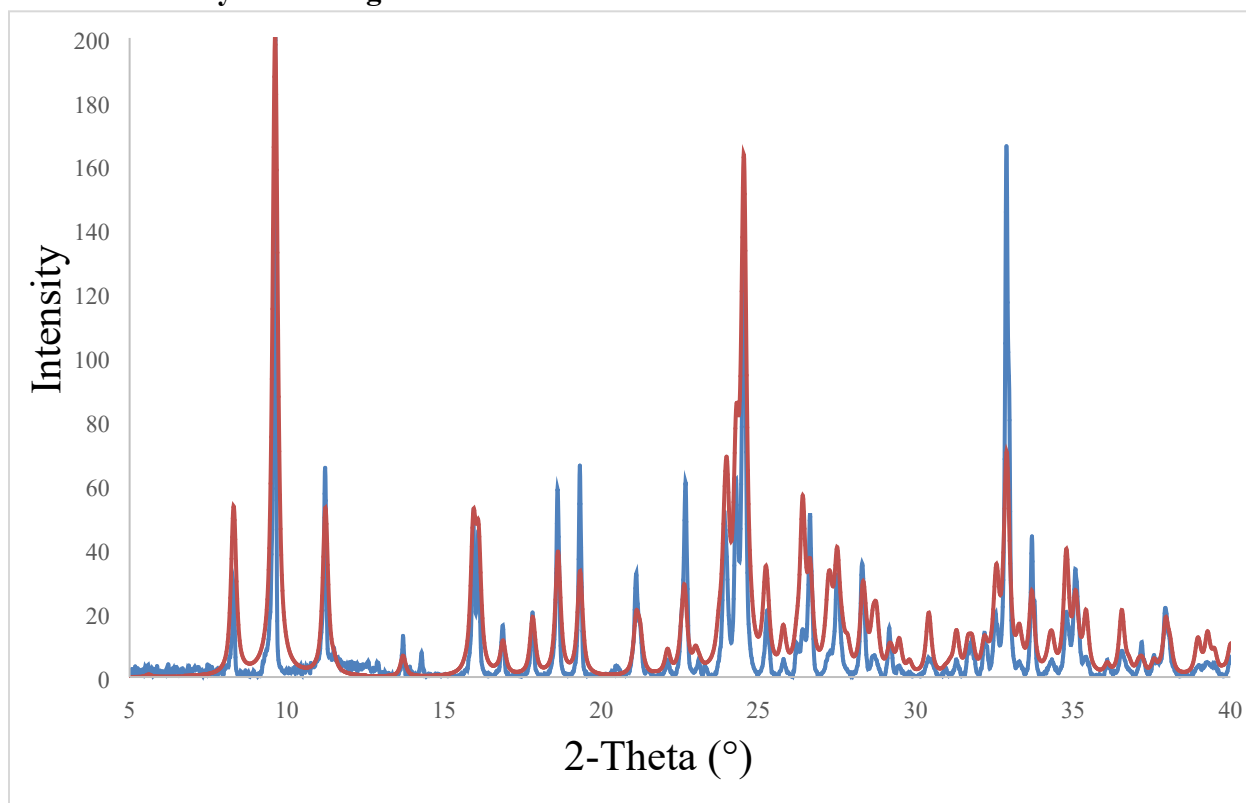


**Figure S3:** Powder X-ray diffraction data for the co-crystal containing both 2(C<sub>6</sub>HICl<sub>4</sub>)•(BPA). Color scheme is the observed pattern (blue) and the calculated powder pattern for 2(C<sub>6</sub>HICl<sub>4</sub>)•(BPA) (orange).



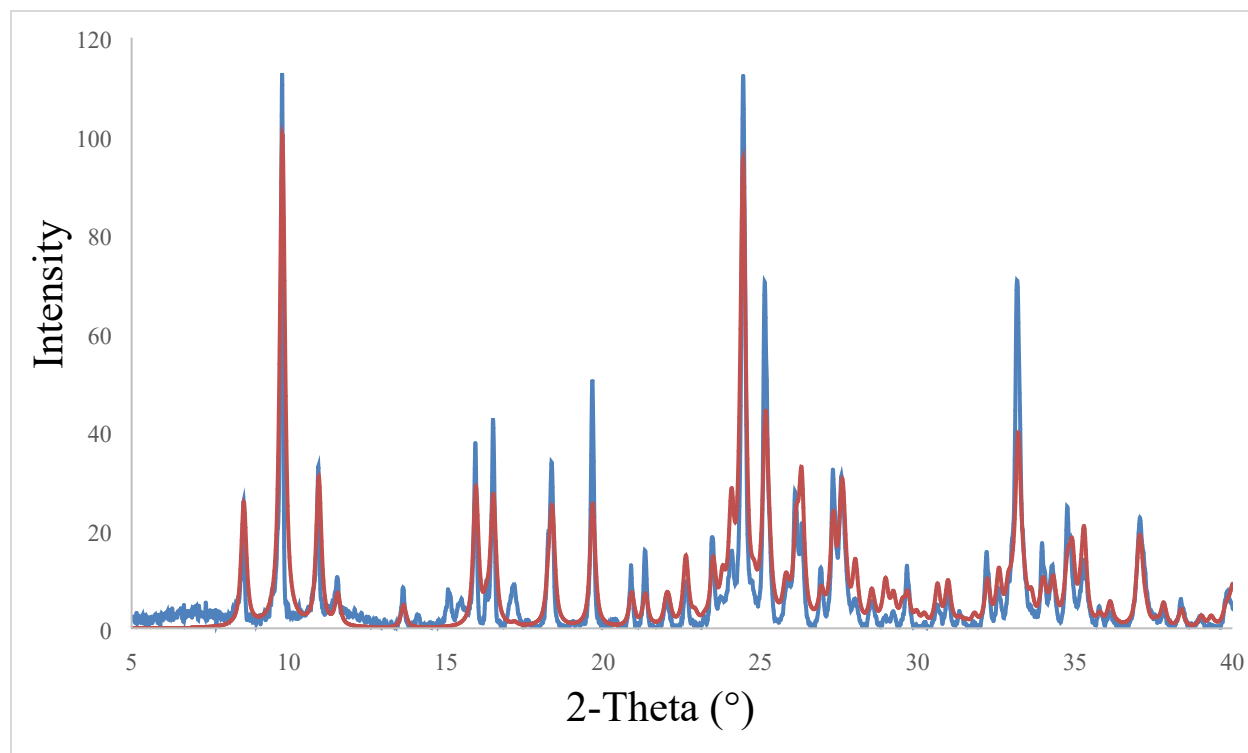


**Figure S4:** Powder X-ray diffraction data for the co-crystal containing both  $2(\text{C}_6\text{H1Cl}_4)\cdot(\text{AP})$ . Color scheme is the observed pattern (blue) and the calculated powder pattern for  $2(\text{C}_6\text{H1Cl}_4)\cdot(\text{AP})$  (orange).

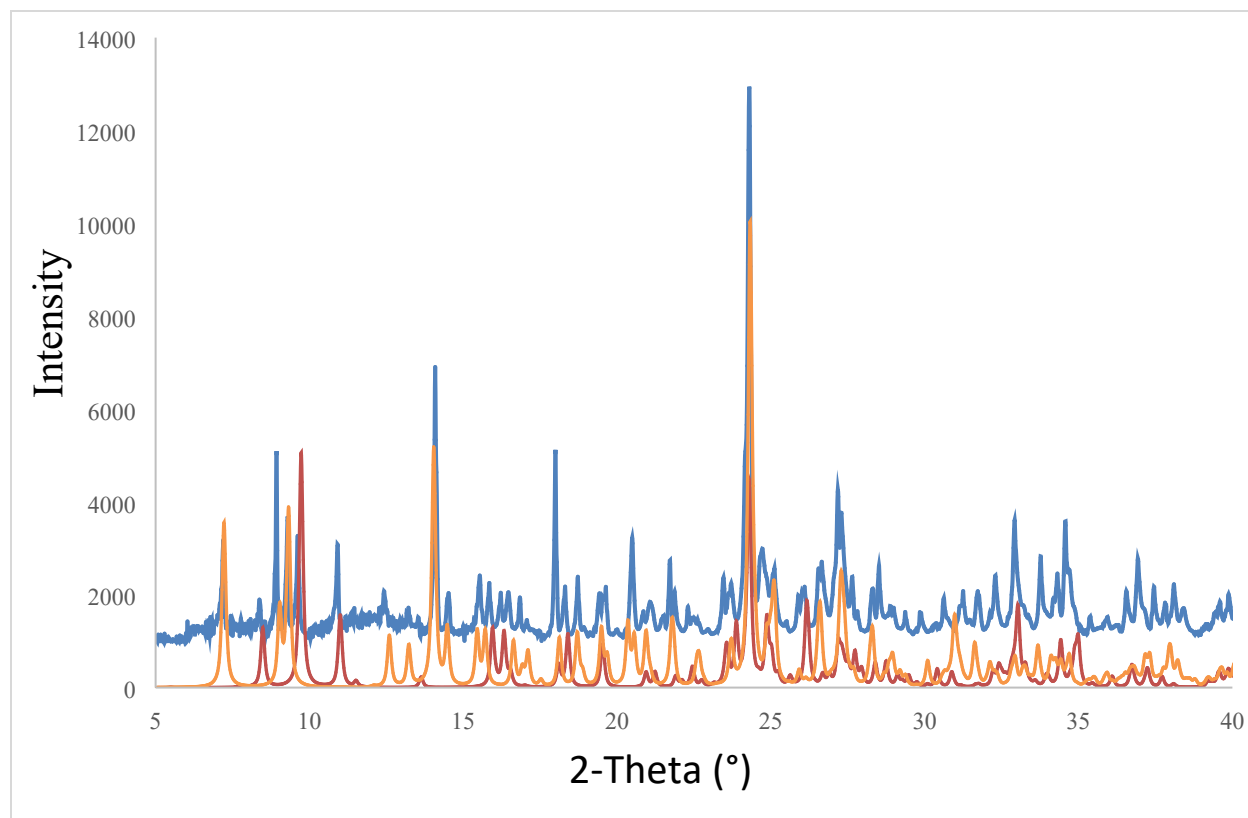


**Figure S5:** Powder X-ray diffraction data for the co-crystal containing both  $2(\text{C}_6\text{H1Cl}_4)\cdot(\text{BPE})$  and  $(\text{C}_6\text{H1Cl}_4)\cdot(\text{BPE})$ . Color scheme is the observed pattern (blue) and the calculated powder pattern for  $2(\text{C}_6\text{H1Cl}_4)\cdot(\text{BPE})$  (orange) and Form I of  $(\text{C}_6\text{H1Cl}_4)\cdot(\text{BPE})$  (green).

## References

1. E. A. Krasnokutskaya, N. I. Semenischeva, V. D. Filimonov, P. Knochel, *Synthesis*, **2007**, 81-84.
2. Gaussian 16, Revision A.03, M. J. Frisch, G. W. Trucks, H. B. Schlegel, G. E. Scuseria, M. A. Robb, J. R. Cheeseman, G. Scalmani, V. Barone, G. A. Petersson, H. Nakatsuji, X. Li, M. Caricato, A. V. Marenich, J. Bloino, B. G. Janesko, R. Gomperts, B. Mennucci, H. P. Hratchian, J. V. Ortiz, A. F. Izmaylov, J. L. Sonnenberg, D. Williams-Young, F. Ding, F. Lipparini, F. Egidi, J. Goings, B. Peng, A. Petrone, T. Henderson, D. Ranasinghe, V. G. Zakrzewski, J. Gao, N. Rega, G. Zheng, W. Liang, M. Hada, M. Ehara, K. Toyota, R. Fukuda, J. Hasegawa, M. Ishida, T. Nakajima, Y. Honda, O. Kitao, H. Nakai, T. Vreven, K. Throssell, J. A. Montgomery, Jr., J. E. Peralta, F. Ogliaro, M. J. Bearpark, J. J. Heyd, E. N. Brothers, K. N. Kudin, V. N. Staroverov, T. A. Keith, R. Kobayashi, J. Normand, K. Raghavachari, A. P. Rendell, J. C. Burant, S. S. Iyengar, J. Tomasi, M. Cossi, J. M. Millam, M. Klene, C. Adamo, R. Cammi, J. W. Ochterski, R. L. Martin, K. Morokuma, O. Farkas, J. B. Foresman, and D. J. Fox, Gaussian, Inc., Wallingford CT, 2016.
3. B. P. Pritchard, D. Altarawy, B. Didier, T. D. Gibson, T. L. Windus, *J. Chem. Inf. Model.* **2019**, *59*, 4814-4820.
4. Spartan'10, Version 1.0.1, Wavefunction, Inc. Irvine, CA, USA.
5. CrysAlis<sup>Pro</sup> (2018) Oxford Diffraction Ltd.
6. R. C. Clark, J. S. Reid, *Acta Cryst.*, *A51*, **1995**, 887-897.
7. O. V. Dolomanov, L. J. Bourhis, R. J. Gildea, J. A. K. Howard, H. Puschmann, *J. Appl. Cryst.*, **2009**, *42*, 339-341.
8. G. M. Sheldrick, *Acta Cryst.*, *A71*, **2015**, 3-8.
9. L. J. Bourhis, O. V. Dolomanov, R. J. Gildea, J. A. K. Howard, H. Puschmann *Acta Cryst.*, *A71*, **2015**, 59-75.